PAN
ARCHIVES OF ACOUSTICS
Vol. **44**, No. 2, pp. 201–214 (2019)
DOI: 10.24425/aoa.2019.126366

Review Papers

Tire and Engine Sources Contribution to Vehicle Interior Noise and Vibration Exposure Levels

Shawki ABOUEL-SEOUD

Faculty of Engineering, El Mataria
Helwan University, Masaken El Helmia
P.O.Box 11718, Cairo, Egypt; e-mail: s_a_seoud@hotmail.com

(*received July 29, 2018; accepted September 12, 2018*)

The main objective of the research presented in this paper is to enhance driver-passengers comfort of a vehicle that in turn leads to better vehicle safety and stability. The focus was put on studying the interior vibration and noise contributions originated from tire-road and engine-transmission subsystems, due to their significant impact on the dynamic performance of the vehicle. The noise and vibration measurements were recorded at the driver's head position and on the driver legs room. Furthermore, the influence of different tire types and road surface textures on the vehicle interior noise and vibration were considered. The results indicate that the widely used conventional engine mounts and tires in commercial vehicles cannot fulfill the conflicting requirements for the best isolation concerning both road surface and engine-transmission induced excitations. The values of driver's head position sound pressure level and floor vibration acceleration broadband averages originate for engine-transmission are lower than that for tire-road interaction. Furthermore, the values of RMS, crest factor, kurtosis and IRI for the vehicle waveform were estimated for vehicle speeds, tire types and road surface textures. Moreover, the percentage contribution for both interior noise and vibration originated from tire-road interaction is higher than the one from vehicle engine-transmission system in all the vehicle speed range, tire type and road surface texture considered.

Keywords: vibro-acoustic; interior vibration; interior noise; tire-road interaction; vehicle engine.

1. Introduction

When driving on road surface, modern vehicles are often sensitive to the interior noise and vibration, occurring in the frequency range of 20–200 Hz. These noise and vibration have a structure-borne origin and are mainly excited by the road roughness and engine unbalancing forces. Moreover, most of these noise and vibration energies are concentrated in 31.5 Hz to 80 Hz third-octave bands. Apparently it was not possible to find any tire with equally good noise and vibration performances in this frequency range.

Nowadays people spend a considerable amount of day-time (10–20%) transfering inside and outside urban environment using different transportation systems (bus, metro, tram, ferryboat, car, train, aircraft). This phenomenon has increased recently due to expansion of cities, mobility demand of poor and do not permit to use the long transfer time for other activities (reading, talking, studying). "All these were usually done in spite of specific targets proposed by the management of poor and do not permit to use the long transfer time for other activities (reading, talking, studying)" (Siano *et al.*, 2015). All these were usually done in spite of specific targets proposed by the management of transportation systems. An overview of investigation studies was presented to assess the problem and recent research projects in this field were discussed.

In a vehicle dynamic system, transmission of sound and vibrations depends on frequency and direction of the input motion and characteristics of the output. It is imperative that automotive manufacturers invest a lot of effort and money to improve and enhance the vibro-acoustics performance of their products. The enhancement effort may be very difficult and time-consuming if one relies only on 'trial and error' method without prior knowledge about the sources (Abouel-Seoud, 2016; Mohammadi, 2015). The vibro-acoustical sources of noise in a passenger vehicle compartment were found. The implementation of spectral analysis method was much faster than the

'trial and error' methods in which parts should be separated to measure the transfer functions. Also by using spectral analysis method, signals can be recorded in real operational conditions which conduce to more consistent results. A multi-channel analyzer was utilized to measure and record the vibro-acoustical signals. Computational algorithms were also employed to identify contribution of various sources towards the measured interior signal. These achievements can be utilized to detect, control and optimize interior noise performance of road transport vehicles.

A-weighted noise levels and sound power are usually applied to measure the noise but they are not adequate to characterize the impact sound inside a vehicle. The most popular approach to determine sound quality of a product is to define an annoyance or specific index (Abouel-Seoud *et al.* 2018; Nor *et al.*, 2008), which involves both subjective and objective evaluations. Subjective and objective tests should be studied concurrently in order to determine the sound quality inside a passenger car. This approach was used in this study to evaluate vehicle comfort index according to the most frequently used sound quality metrics, namely Zwicker loudness, sharpness, roughness and fluctuation strength. As a result, researchers of different fields of automotive acoustics investigations can use this index according to the type of road (international road roughness) without any need to perform time-consuming jury tests (Mahajan, Rajopadhye, 2013). The metrics were correlated with jury test results that show which of them and how much had affected the acoustical comfort of the vehicle.

Sound transmission into a vehicle was classified as either airborne or structure-borne sound, where coherence function analysis is often used to identify transmission paths. However, it can be difficult to separate the airborne from structure-borne components (Kim, 2000; Mohamed *et al.*, 2017). The principle of acoustic reciprocity offers a convenient method for overcoming this difficulty. The principal states that the transfer function between an acoustic volume velocity source and an acoustic receiver is independent of a reversal of the position of source and receiver. A stationary tire was excited and the surface velocity of the tire was measured at a number of discrete points. Two sets of measurements were then combined to yield a measure of the sound pressure due to a point force on the tire via the acoustic transmission path only. This technique also provides information on the relative contributions of various regions of the tire wall to the resultant noise.

Ride comfort in road vehicles is related to vehicle vibration levels and the perception of passenger fatigue. Vibration in vertical direction on the seat and floor was measured to characterize the ride comfort based on standard formulae and frequency analysis. A mid-size saloon vehicle and an off-road vehicle were driven on smooth, spalled and coarse asphalt road surfaces. To assess the vertical vibrations transmitted to the passengers, vibration dose values, kurtosis, frequency response functions and power spectral densities of the compartment recorded signals were evaluated (Abouel-Seoud, 2014). Seat effective amplitude transmissibility value based on vibration RMS and vibration dose values were also evaluated. The results indicate that the vibration dose value increases in proportion to the vehicle speed and road roughness.

Vehicle acoustical comfort and vibration in passenger car cabin are the factors which attract the buyers as they guarantee comfortable driving environment. The amount of discomfort depends on the magnitude, frequency, direction and also the duration of exposed vibration in the cabin. Generally the vibration is caused by two main sources, i.e. engine transmission and interaction between tires and the road surface. The comfort of the driving affects the drivers by influencing their performance by bothering vision (Junoh *et al.*, 2012a), and at the same time giving stress to the driver due to generated noise. A research was carried out to find the amount of noise influenced by the vibration due to interaction between tires and road surface (Junoh *et al.*, 2012b). The sound quality analysis was focused on the estimation of the noise changes through the generated sound quality depending on engine speeds, where the amount of sound quality is followed by the increase and decrease of the engine speeds. A technical method was provided to show the correlation between generated noise sound quality and the exposed vibration caused by the interaction between tires and road surface.

The transient vibration phenomenon in a vehicle powertrain system during the start-up (or shut-down) process was studied in (Li, Singh, 2015) with focus on the development and experimental validation of the nonlinear powertrain models. First, a new nonlinear four-degree-of-freedom torsional powertrain model for this transient event, under instantaneous flywheel motion input, was developed and then validated with a vehicle start-up experiment. Second, the interactions between the clutch damper and the transmission transients were established via transient metrics. Third, a single-degree-of-freedom nonlinear model, focusing on the multi-staged clutch damper, was developed and its utility was then verified.

Coast-down modelling has been widely used to assess vehicle aerodynamic drag and rolling resistance by fitting a vehicle resistance model to speed measurements and thereby get an estimate on model parameters (Andersen, Larsen, 2015). A coast-down model was used for assessing how road surface characteristics influence rolling resistance. Parameter estimation as well as an extensive perturbation analysis of the parameter fit with respect to data noise was performed. Functional Data Analysis (FDA) was introduced and discussed as a tool for this. It was concluded that

FDA was a powerful tool for (1) approximating derivatives, (2) assessing the degree of smoothing of the data, (3) handling noise sources in the perturbation analysis, and (4) enabled numerical solutions of the coast-down Ordinary Differential Equation (ODE) model.

Assessment and evaluation of vehicle low frequency interior noise, infrasound closer to the threshold of hearing and their potential effects on human health were presented in (Abouel-Seoud, 2015). The vehicle interior noise of off-road and mid-size vehicles was measured while driving on three different asphalt road surfaces. The vehicle acoustic comfort factor (VACF) was found to be at lower level for a relatively high acoustical comfort. Furthermore, at constant vehicle speed, the kurtosis parameter value was greater in high roughness road surface and was proportional to vehicle speed for every kind of road surface. Kurtosis has inverse effect on the VACF value. The VACF for road surface with higher roughness was lesser than the VACF for smoother road surface at same vehicle speed.

To reduce vibration and noise transmissions from a source to vehicle passenger's cabin many viscoelastic joints has been used such as engine mounts and bushings. The amount of stiffness fluctuation of engine mounts due to material uncertainty and environmental temperature variation was estimated using a statistical approach. First, the dynamic characteristics of engine mounts were described by fractional derivative model (van der Seijs *et al.*, 2016). The fractional-derivative-model parameters and statistical information of a rubber were estimated from the test data. To estimate the variability of the dynamic characteristics of the engine mount due to the uncertainties of the rubber, the Monte Carlo simulation was used (Sun *et al.*, 2016). Operational conditions such as temperature are also included in the variability analysis. The variability analysis results show that the dynamic stiffness variation of the engine mount due to the uncertain material properties of the rubber is more than 10 dB at 100 Hz.

The above mentioned papers have shown that the efforts which had been done for studying the vibration and noise phenomena inside the vehicle cabin were used the whole vehicle system with the traditional analysis techniques, their contributions were limited due to the mixed data obtained which affected the success of these techniques. The vehicle interior vibration and noise originate from the individual vehicle subsystem such as tire-road and engine-transmission separately have been given little consideration. However, the objective of this paper is to estimate the contribution of tire-road and engine-transmission as a separate vehicle sub-system on the whole vehicle interior vibration and noise. The vehicle interior vibration measurements were done on the vehicle floor at the driver's legs room, while the interior sound pressure level was measured at the driver's head position. The test vehicle was a mid-size executive vehicle, and was driven at speed started from 20 km/h to 100 km/h. Furthermore, the influence of different tire types and road surface textures on vibration level was investigated.

2. Vehicle sources setup

2.1. Complete (whole) vehicle sources

The objective of the field campaign was to analyze contributions of whole vehicle sources to its interior vibration and noise. The test vehicle was a mid-size executive vehicle, with a 4-cylinder engine. It is a four-door sedan with a curb weight of 1162 kg and Lotus-tuned suspension settings, the vehicle handles well through tight corners and is a good high-speed cruiser. The dimensions specifications of the vehicle body and vehicle chassis specifications are tabulated in Tables 1 and 2, respectively. The road-test mode was employed in the present experimental work. The vehicle is equipped with microphone, accelerometers, labshop and analyzer. Vehicle speed was recorded during the test. In this case, the vehicle interior noise and vibration generated from all the vehicle sources during the driving were measured.

Table 1. Vehicle body specifications.

Vehicle body	Dimensions
Wheelbase	2.55 m
Track (front/rear)	1.569 m/1.588 m
Length	4.120 m
Width	1.79 m
Height	1.61 m
Ground clearance	0.165 m
Headroom (front/rear)	1.02 m/1.006 m
Shoulder room (front/rear)	1.402 m/1.40 m
Legroom (front/rear)	1.069 m/0.991 m
Hip room (front/rear)	1.35 m /1.338 m
Passenger volume	2.65 m^3

Table 2. Vehicle chassis specifications.

Vehicle chassis	Specifications
Vehicle class	Midsize sedan
Layout	Front engine, front-wheel drive
Front suspension system	Independent, MacPherson strut, stabilizer bar, gas-filled shock absorbers
Rear suspension	Torsion beam, gas-filled shock absorbers
Steering type	Rack and pinion, electric power steering

2.2. Vehicle engine-transmission source

The contribution analysis of the vehicle various sources for the vehicle interior vibration and noise, with a main focus on the source of the engine-transmission was conducted. The vehicle interior vibration acceleration and sound pressure level were measured when the vehicle was lifted up from the ground to release the contact between the tires and the ground. This was done to eliminate the influence of tire-road interaction effects. The vehicle was then taken under a run up test from 1250 rpm (20 km/h) to 6250 rpm (100 km/h) throughout the measurements presented herein. The gear shifts of the transmission can be selected manually to allow measurements over the whole rotational-speed (rpm) range without gear shift change. To alter the excitation of the system, engine control units (ECU), with different parameter sets, were available for the measurements. Table 3 presents the vehicle power-train specifications.

Table 3. Vehicle power-train specifications.

Element	Specifications
Type	1.6L, 4-cylinder, aluminum block and head
Valve System	Dual Continuously Variable Valve Timing (CVVT)
Displacement (cc)	1,591 cc
Compression ratio	11.0:1
Horsepower (SAE net)	138 hp @ 6,300 rpm
Torque (SAE net)	165 N·m @ 4,850 rpm
Fuel System	gasoline direct injection
Transmission	5-speed manual, electronically controlled

2.3. Vehicle tire-road interaction source

The contribution analysis of the vehicle various sources for the vehicle interior vibration and noise, with a main focus on the source of the tire-road interface was conducted. The vehicle interior vibration acceleration and sound pressure level were measured when the vehicle noise and vibration originate during the vehicle coast down conditions with engine unloaded (neutral gear) were conducted as a good representative tire-road interface source of strong low frequency noise.

As shown in Table 4, the selected road surface textures were asphalt, sand and gravel and their characteristics are also presented in Table 4. The asphalt had a flat, smooth surface and occasional unevenness, which resulted in minimum disturbances. The tire types and their technical specifications are shown in Table 5.

This was done to eliminate the influence of engine-transmission effects. The vehicle was then taken under a run up test from 1250 rpm (20 km/h) to 6250 rpm (100 km/h). The gear shifts of the transmission can be selected manually, to allow measurements over the whole rotational-speed (rpm) range without gear shift change.

Table 4. Description of road surface textures.

Type of road	Road surface appearance	Road surface characteristics	Road surface texture
Smooth Asphalt	Smooth asphalt, no wear or weathering, small stones	Low overall level, higher frequency greater proportion of noise, no “roar”	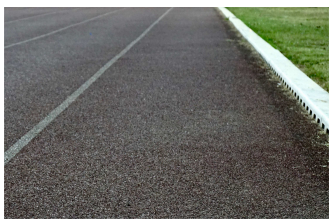
Sand	Sand soils and size distribution of the fine sand and greater porosity	Are often dry, nutrient deficient and fast-draining, water retention and resistance to penetration, they exhibit lower permeability	
Gravel	Pattern not complete random, polished stones, moderately	High max stone size, high overall level	

Table 5. Tires technical specification.

Technical details	Data		
Brand	Bridgestone	Bridgestone	Bridgestone
Description	 185/65 R15 88H	 195/60 R15 88H	 195/65 R15 91H
Model	B250	AR20 (Original)	ER-300
Item weight [kg]	8 kg	8 kg	8 kg
Tyre Type	Tubeless Type	Tubeless Type	Tubeless Type
Circumference [mm]	1952.5	1932	1993.34
Radius [mm]	310.75	307.5	317.25
Sidewall height [mm]	120.25	117	126.75
Overall diameter [mm]	621.5	615	634.5
Section width [mm]	185	195	195
Aspect ratio [%]	65	60	65
Construction	R	R	R
Rim diameter [mm]	381	381	381
Load index rating	88	88	91
Load carrying capacity [kg]	560	560	615
Max. speed [km/h]	210	210	210

3. Measurement procedures

3.1. Test setup

The vehicle has a four cylinder engine of 1.6 liters. The engine and the transmission are installed on the vehicle body by three mounts. The test setup was started by using two accelerometers, one mounted on the top of vehicle engine as shown in Fig. 1, while the other is mounted on the vehicle floor as shown in Fig. 2. These mounting condition is one of the most critical factors in achieving accurate results, where poor attachment reduces the mounted resonance frequency and severely limits the useful frequency range of the accelerometer. Epoxy hard glue only slightly reduces the resonance frequency and was a good choice for measurement in moving condition. Triboelectric noise was prevented by using low noise cables which were fixed to the structure by adhesive tape. The excitation sources of tire/road and engine-transmission were

Fig. 1. Position of the accelerometer over the top of the vehicle engine.

Fig. 2. Accelerometer positions on vehicle floor.

considered. One microphone was positioned at the vehicle driver's head position, i.e. the microphone was positioned close to the head, in order to analyze the effect of the noise on the driver while driving the vehicle. The vehicle was driven under the conditions of coast down driving (which is a standard driving test) to eliminate the influence of vehicle engine. Microphone was placed nearly horizontally, with its maximum sensitivity direction as shown in Fig. 3. Figure 4 depicts the analysis instrumentation system used in the measurements. To eliminate the influence of tire/road interaction, the vehicle was lifted up from the ground to release the contact between the tires and the ground.

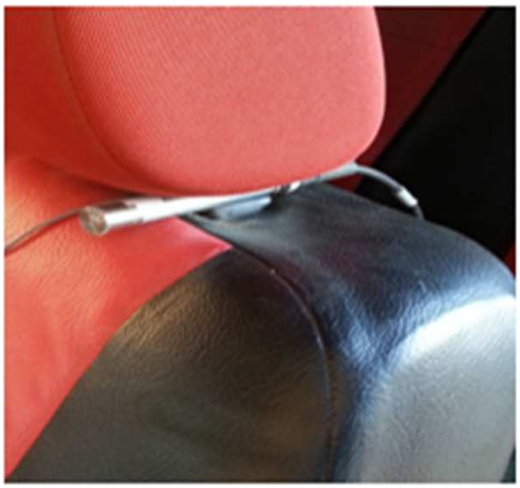

Fig. 3. Position of the microphone.

Fig. 4. Analysis instrumentation system.

3.2. Vehicle interior noise measurement

Vehicle interior noise originates during the coast down driving test. The A-weighting of the dB sound pressures level reveals tonal aspects (speed dependent) related to tire rotation frequency as well as constant resonance characteristics.

During the measurements the vehicle was driven on the road surfaces textures with minimal traffic as shown in Table 4, i.e. the aim was to minimize the influence of other sources of vibration and noise from passing vehicles. The measurements were done at various vehicle speeds from 20 km/h to 100 km/h.

Noise originated during driving vehicle coast down tests with engine unloaded (neutral gear) were conducted as a good representative source of strong low frequency noise. Under the conditions of this type of test, engine – transmission source was illuminated. During the measurements, the vehicle was driven on the road surfaces with minimal traffic, i.e. the aim was to minimize the influence of other sources of vibration and noise from passing vehicles. The tires technical specifications are tabulated in Table 5. The A-weighting of the dB sound pressures level reveals tonal aspects (speed dependent) related to tire rotation frequency as well as constant resonance characteristics. To measure vehicle interior noise characteristics up to 400 Hz, the relevant physical effects have to be considered. Three main groups of vehicle areas interacting with one another and influencing the interior noise can be selected. These are, the vehicle body structure itself, the fluid enclosed in the passenger room (as well as other cavities, e.g. cavities behind covers) and the trim parts connected to the vehicle body. In the present work, one vehicle was prepared from the point interior noise using a recording technique with a signal length of 0.8 seconds and a sampling rate of 2048 Hz. Under each working condition, the noise signals levels were measured and analyzed in terms of sound pressure level (SPL) by 1/2-in condenser microphone Bruel & Kjaer, Type 4189-A-021 with all vehicle windows closed. The analysis was carried out by using the a Bruel & Kjaer portable, multichannel PULSE, Type 3560- B-X05 analyzer, Bruel & Kjaer PULSE labshop, and the measurement software type 7700. The measurements data were saved in the computer. During measuring, the microphones were arranged at 0 or 0.2 meters distance from the centerline of the seats with a height of 0.7 meters, depending on the seated conditions.

3.3. Vehicle floor vibration measurement

The vibration measurements were made where the vibration samples were acquired with integration period of 0.8 second. The vibration acceleration signals were measured in vertical direction by using Bruel & Kjaer accelerometer Type 4514B-001 mounted upon the top of the vehicle engine and the vehicle floor in legs room. The vibration amplitudes recorded from the vehicle engine and floor during tests were conducted for possible artifacts and any unclear signals detected were removed.

3.4. International roughness index (IRI) measurement

There are three main sources of vibration transmitted to the vehicle passengers: road roughness, vehicle suspension and driver's behaviour (including choice of speed). Within reasonable variations in these factors, road roughness plays a considerably greater part than the other two. In vehicle research into acoustic quality, all of the three sources play an important role. In order to include the road roughness in this study, the International Roughness Index (IRI) was used. It is a general pavement condition indicator that summarizes the roughness qualities which affect vehicle response and is most appropriate when a roughness measure was desired that relates to overall ride quality and overall surface conditions. Many attempts have been made to find out the international index defining the roughness of the road.

Engineers use road profilers (road meter system) for IRI measurement. The key importance of IRI is that road profiler users have shared experiences measuring IRI. As shown in Fig. 5, it is a quarter (one corner) of the vehicle system, which includes one tire and axle, suspension spring, and damper. It accumulates suspension motion while travelling over the road. Roughness is measured as the accumulated suspension stroke normalized by the total travelled distance. IRI is usually presented in engineering units such as mm/m, m/km, or inc/mile. It is highly correlated with acceleration of vehicle passengers (ride quality) and tire load (vehicle controllability). Roads around the world may have different names and visual characteristics, but researchers can compare vibration analyses results for roads with similar IRI (Nahvi *et al.*, 2009).

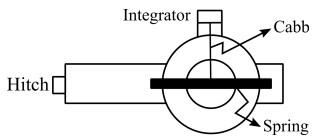

Fig. 5. Schematic of a road profiler.

3.5. Experimental error estimation

Errors and uncertainties in the experiments may result from instrument selection, condition, calibration, environment, observation, reading, and test planning. Uncertainty analysis is needed to prove the accuracy of the experiments. An uncertainty analysis was performed using the method described by (Gallo *et al.*, 2009). Percentage uncertainties of various parameters like vehicle road torque, vehicle road power, vehicle road acceleration time, acceleration distance, and speed were calculated using the percentage uncertainties of various instruments. Total percentage uncertainty of these experiments for the whole experiment is obtained to be ±3.2%.

4. Vibration waveform processing data

4.1. Root mean square (RMS)

RMS is a kind of average of signal, for discrete signals, the RMS value is defined as:

$$\mathrm{RMS} = \sqrt{\frac{1}{N}\sum_{n=1}^{N}(x(n)-\overline{x})^2}, \quad \overline{x} = \frac{1}{N}\sum_{n=1}^{N}x(n), \tag{1}$$

where N is the number of data points taken in the signal, $x(n)$ is the amplitude of the signal at the n-th point, and $\overline{x}$ is the mean value of all the amplitudes.

4.2. Kurtosis of vibration signals

Kurtosis is the fourth statistical moment signal, known as a global statistical parameter that is highly sensitive to the impulsiveness of the time-domain data. For discrete data sets it can be approximated by

$$K = \frac{1}{n\sigma^4}\sum_{j=1}^{n}(x_j-\overline{x})^4, \tag{2}$$

where K is kurtosis, n is the number of discrete data, σ is the standard deviation, x_j is any data, and $\overline{x}$ is the average of total data. The kurtosis value is approximately 3.0 for a Gaussian distribution. Higher kurtosis indicates the existence of numerous extreme data values, inconsistent with a Gaussian distribution, while lower than 3.0 designates a relatively flat distribution (Mahajan, Rajopadhye, 2013).

4.3. Crest factor

The crest factor CF is defined as the ratio of the peak value PV to the RMS of the signal. The factor corresponds to the ratio between the crest value CV (maximum absolute value reached by the function representative of the signal during the considered period of time) and the root mean square (RMS) value (efficient value) of the signal:

$$\mathrm{CF} = \frac{\mathrm{PV}}{\mathrm{RMS}} = \frac{\mathrm{CV}}{\mathrm{RMS_{Value}}} = \frac{\sup|x(n)|}{\sqrt{\frac{1}{N}\sum_{n=1}^{N}[x(n)]^2}}, \tag{3}$$
$$\mathrm{PV} = \mathrm{CV} = \frac{1}{2}[\max(x(t)) - \min(x(t))],$$

where N is the number of samples taken within the signal and $x(n)$ the time domain signal.

5. Results and discussion

The vehicle interior noise and vibration which are heard and felt respectively by the occupants of a vehicle primarily originates from (a) the engine, transmission system and accessories, (b) tire/road excitation,

and (c) aerodynamic excitation. The contribution of aerodynamic noise is not very great at moderate vehicle speeds and even at high speeds it seldom becomes a dominant source, and thus is not considered in this study.

5.1. Vehicle engine vibration characteristics

The vehicle was taken under a run up test from 1250 rpm (20 km/h) to 6250 rpm (100 km/h). One accelerometer was mounted on the top of the engine as shown in Fig. 1, where the vibration acceleration was measured. This represents the engine source. Sample from the vibration measurement results at speed of 2150 rpm (80 km/h) for time history and frequency-domain are shown in Figs 6 and 7 respectively. The vibration acceleration measured was truncated to show the frequency range of interest which is up to 400 Hz.

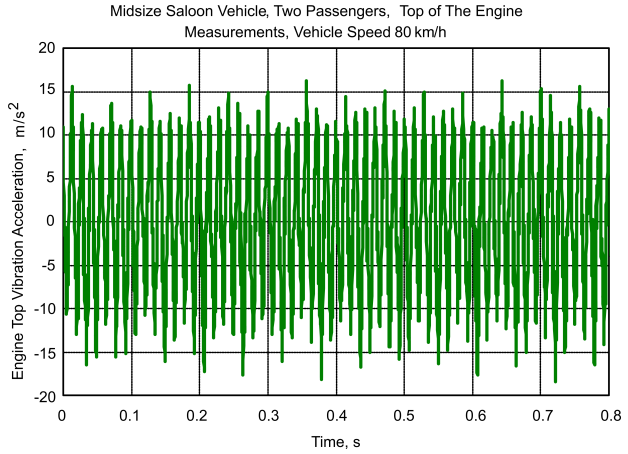

Fig. 6. Time history of the engine vibration acceleration at 2150 rpm (80 km/h).

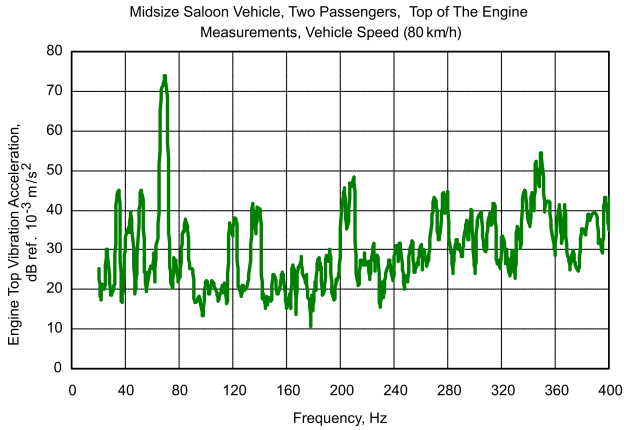

Fig. 7. Frequency-domain of the engine vibration acceleration at 2150 rpm (80 km/h).

5.2. Vehicle floor vibration waveform results

One accelerometer was mounted on the vehicle floor (as a receiver) in the center point of the driver' legs room as shown in Fig. 2. This point was chosen to be the vibration measurement point, where the driver spends a lot of time while driving. As an example of vehicle floor of the experimental raw waveform data of the vibration acceleration in terms of time history for engine, tire/road and complete (whole vehicle) sources at vehicle speed of 80 km/h are shown in Figs 8 to 10 respectively.

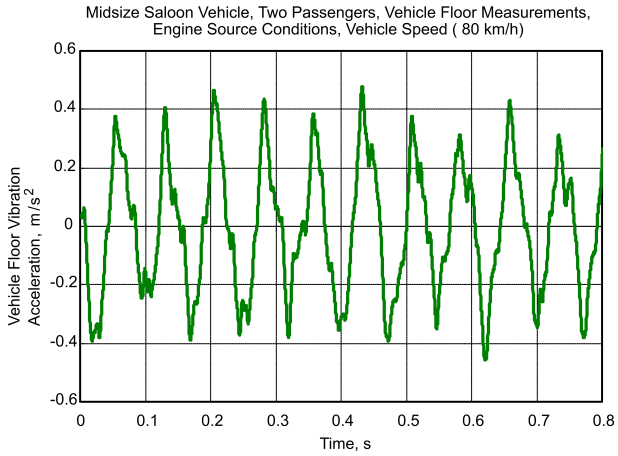

Fig. 8. Vehicle floor vibration acceleration originates from engine source condition at vehicle speed 80 km/h.

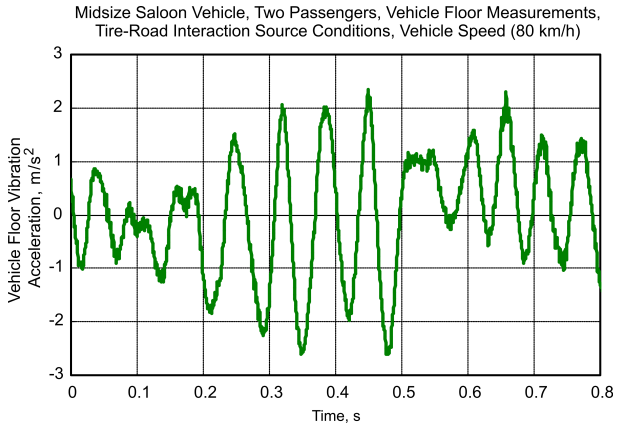

Fig. 9. Vehicle floor vibration acceleration originates from tire-road source condition at vehicle speed 80 km/h.

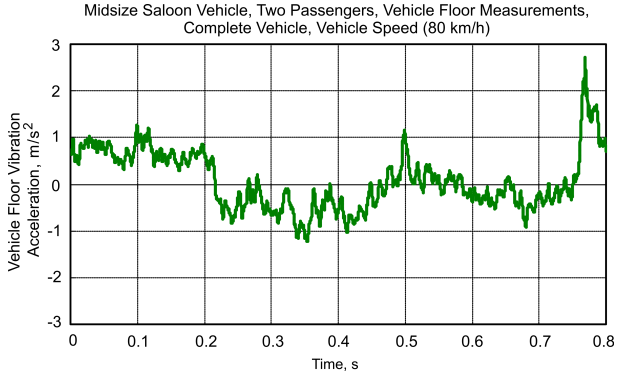

Fig. 10. Vehicle floor vibration acceleration originates from whole vehicle sources condition at vehicle.

The root mean square (RMS), kurtosis (K) and crest factor (CF) are computed based on Eqs (1) to (3) respectively, and the international road roughness (IRI) which was measured based on the measurement methodology presented in Subsec. 3.5. Referring to Table 6, where the vehicle floor vibration waveform data computed values of RMS, Kurt, CF and IRI are tabulated at different vehicle speeds. As an example, the vehicle speed of 80 km/h, tire type of 195/60 R15 88H and asphalt road surface texture the RMS values are 1.09 m/s^2 (whole vehicle), 0.224 m/s^2 (engine-transmission), and 0.63 m/s^2 (tire/road). According to the data presented in the Table, it can be observed that the CF values are ranged 1.64 and 4.33. Kurt values are ranged 1.94 and 4.57. It is known that higher kurtosis indicates the existence of numerous extreme data values, inconsistent with a Gaussian distribution, where the kurtosis value approximately 3.0. Moreover, the IRI values are ranged between 8.61 (20 km/h) and 2.09 (100 km/h) and these values are proportional to kurtosis values which indicate that human perceives more peaks and impulses when driving on road surfaces with greater roughness.

Table 7 presents the influence of tire and road surface textures types on vehicle floor vibration waveform data at the vehicle speed of 80 km/h with different tire and road surface texture types for the individual sources (complete vehicle, engine and tire-road) for tire type of 195/60 R15 88H, at asphalt road surface texture and the lowest RMS value is 0.71 m/s^2 (whole vehicle), 0.22 m/s^2 and 0.45 m/s^2 (tire/road). On the other hand, the asphalt road surface texture shows the lowest RMS value when compared with the other road surfaces, where the highest RMS value was recorded for the sand surface texture. The values of CF with respect to the type of tires and road surface textures are ranged between 2.03 and 4.46. It should be borne in mind, that the normal distribution has either kurtosis or crest factor value of 3, which is a good condition.

5.3. Vehicle floor vibration acceleration results

For a vibratory system the response in terms of vibration amplitude is dependent on both the exciting force and the dynamic characteristics of the system. The emitted noise on the other hand also depends on the size of the vibratory system in relation to the frequency of vibration. A vehicle has two primary sources of excitation: (a) the engine and its transmission system; (b) the tire-road surface interaction. All road surfaces have a random profile and the tires and suspension system convert this into a random vibration input to the body structure as another major source of excitation. This excitation is of high

Table 6. The influence of vehicle speeds on the floor vibration wave form data for midsize saloon vehicle and two passengers.

Vehicle speed [km/h]	Individual sources											
	Whole vehicle				Engine				Tire-road			
	RMS	IRI	CF	Kurt	RMS	IRI	CF	Kurt	RMS	IRI	CF	Kurt
20	0.32	2.09	2.72	1.96	0.043	–	2.86	3.10	0.17	2.09	2.90	3.21
40	0.41	3.61	2.91	2.85	0.145	–	2.05	2.03	0.24	3.61	2.98	2.74
60	0.91	6.57	2.87	2.80	0.155	–	2.32	1.97	0.25	6.57	2.52	2.56
80	1.09	6.81	4.33	3.29	0.224	–	2.10	2.06	0.63	6.81	2.10	2.30
100	1.54	8.61	3.61	4.57	0.581	–	1.87	1.94	0.59	8.61	1.64	2.87

Table 7. The influence of vehicle tire type and road surface texture on the floor vibration waveform data for midsize saloon vehicle and two passengers.

Road/tire parameters	Individual sources											
	Whole vehicle				Engine				Tire-road			
	RMS	IRI	CF	Kurt	RMS	IRI	CF	Kurt	RMS	IRI	CF	Kurt
Tire type	Speed, 80 km/h, asphalt road surface texture											
185/65 R15 88H	1.09	6.8	4.33	3.30	0.22	–	2.1	2.06	0.63	6.80	2.10	2.30
195/60 R15 88H	0.71	5.3	4.23	3.50	0.22	–	2.1	2.06	0.45	4.40	2.40	3.10
195/65 R15 91H	0.96	5.5	4.46	3.10	0.22	–	2.1	2.06	0.55	4.40	2.50	2.30
Road surface texture	Speed, 80 km/h, tire type 185/65 R15 88H											
Asphalt	1.09	6.8	4.33	3.30	0.22	–	2.1	2.06	0.63	6.81	2.10	2.30
Sand	7.54	2.8	2.89	4.50	0.22	–	2.1	2.06	0.45	47.10	7.90	33.90
Gravel	1.17	7.3	2.64	3.17	0.22	–	2.1	2.06	0.17	1.08	2.03	2.29

amplitude with a very wide spectrum and frequencies up to 400 Hz. Figure 11 shows an example of the time history of the vehicle floor vibration acceleration (FVA) spectra, while Fig. 12 shows frequency domain comparatively presenting raw for the complete (whole) vehicle, engine-transmission and tire-road interaction sources at vehicle speed 80 km/h (5000 rpm). It is observed that the FVA originates from the tire-road interaction sources is higher than that originates by engine-transmission sources and both are less than that for complete (whole) vehicle sources in the whole frequency range.

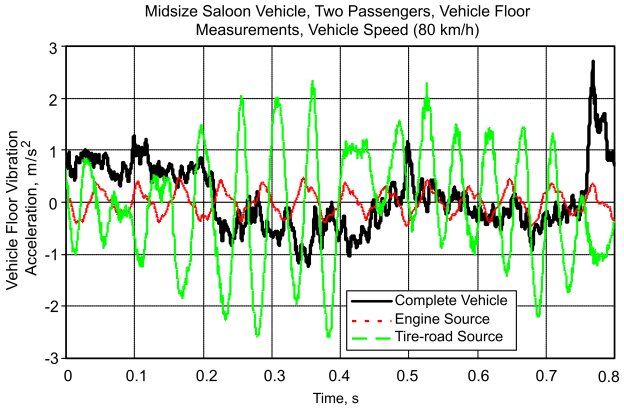

Fig. 11. Time history of floor vibration acceleration (FVA).

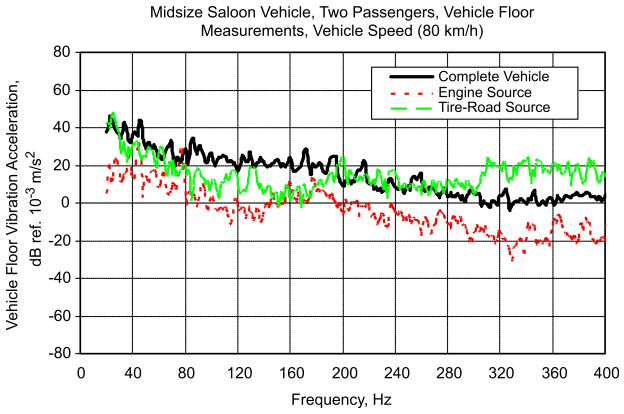

Fig. 12. Frequency-domain of floor vibration acceleration (FVA).

5.4. Vehicle interior noise results

Noise inside a car is produced by complex vibrations of all the body surfaces enclosing the car interior. Vibrations of these surfaces are caused by (a) direct transmission of vibratory forces from the engine or the road into the vehicle structure, which are subsequently transmitted to the body surfaces and (b) by airborne noise from the engine, which also causes the body surfaces to vibrate and produce noise inside the passenger compartment. The characteristics and level of the resultant noise are determined not only by the characteristics of the exciting forces (spectra of engine force, road excitation and airborne noise), but also by the elastic properties/dynamic characteristics of the vehicle structure and the interior body surfaces, all of which have a large number of natural modes of vibration. Furthermore, resonances in the air inside the car cavity also have a significant effect and can modify the characteristics of noise and increase its level. On the other hand, the noise inside a vehicle is complex by nature, because it consists of both random background noise (originating mainly from road surfaces) and discrete frequency components (originating from the engine) superimposed on the background noise.

Figure 13 shows an example of the time history of the vehicle cabin interior sound pressure level (SPL) spectra, while Fig. 14 shows the corresponding frequency-domain for the complete (whole) vehicle, engine-transmission and tire-road interaction sources at vehicle speed 80 km/h (5000 rpm). It is observed that the SPL originates from the tire-road interaction sources is higher than that originates by engine-transmission sources and both are less than that for complete (whole) vehicle source in the whole frequency range. From all the spectra and in low frequency range below 500 Hz, the interior SPL dominate by the acoustic cavity modes and start to converge roughly above 400 Hz. The results indicate that the widely used con-

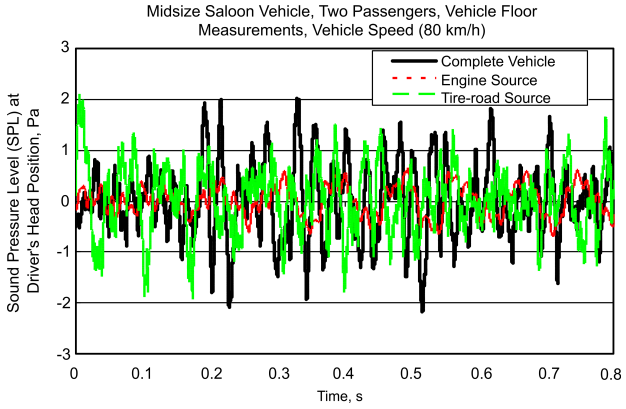

Fig. 13. Time history of vehicle interior sound pressure level (SPL).

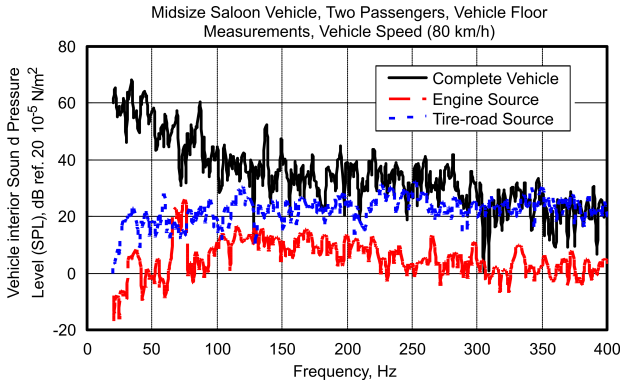

Fig. 14. Frequency-domain of vehicle interior sound pressure level (SPL).

ventional engine mounts and tires in commercial vehicles cannot fulfill the conflicting requirements for the best isolation concerning both road surface and engine-transmission induced excitations. Moreover, it is mainly observed from 20 Hz to 100 Hz, where most of these noise and vibration energies are concentrated. Apparently it was not possible to find any tire with equally good noise and vibration performances in this frequency range.

5.5. Source contribution level

The noise and vibration which are heard and felt by the occupants of a vehicle primarily originate from (a) the engine, transmission system and accessories, (b) road excitation, and (c) aerodynamic excitation. The contribution of aerodynamic excitation is not very great at moderate speeds and even at high speeds it seldom becomes a dominant source, and thus is not taken into consideration. However, evaluation of the contribution of items (a) and (b) stated above can be made by using the broadband averages computed from frequency-domain spectra collected in Tables 8 to 11 and substituted in the relation presented in Appendix. The results presented in Tables 8 and 9 indicate the broadband averages of interior sound pressure level (SPL) measured and computed for whole vehicle sources, engine-transmission and tire-road interaction sources for the vehicle speed of 20 km/h to 100 km/h (Table 8), road surface textures and tire types (Table 9) respectively. On the other hand, the results presented in

Table 8. The influence of vehicle speeds on SPL percentage contribution measured at the driver's head position for midsize saloon vehicle and two passengers.

Vehicle speed [km/h]	Sound Pressure Level (SPL), Pa(A) (dBA ref. $2{\cdot}10^{-5}$ N/m^2)				
	Whole vehicle	Individual sources			
		Engine	Percentage contribution	Tire-road	Percentage contribution
20	0.012 (55.563)	0.0015 (37.501)	12.50	0.0047 (47.421)	39.17
40	0.013 (56.258)	0.0024 (41.584)	18.46	0.0076 (51.596)	58.46
60	0.0135 (56.586)	0.00242 (41.656)	17.93	0.0060 (49.542)	44.44
80	0.0233 (61.322)	0.0025 (41.938)	10.73	0.0133 (56.456)	24.40
100	0.042 (66.444)	0.0042 (46.444)	10.00	0.0139 (56.840)	12.72

Table 9. The influence of vehicle tire and road surface types on SPL percentage contribution measured at the driver's head position for midsize saloon vehicle and two passengers.

Road/tire parameters	Sound Pressure Level (SPL), Pa(A) (dBA ref. $2{\cdot}10^{-5}$ N/m^2)				
	Whole vehicle	Individual sources			
		Engine	Percentage contribution	Tire-road	Percentage contribution
Tire type	Speed, 80 km/h, road surface texture asphalt				
185/65 R15 88H	0.0233 (61.322)	0.0025 (41.938)	10.73	0.0133 (56.456)	24.40
195/60 R15 88H	0.0490 (67.784)	0.0025 (41.938)	5.10	0.0390 (65.80)	79.59
195/65 R15 91H	0.0644 (70.157)	0.0025 (41.938)	3.88	0.0544 (68.69)	84.47
Road surface texture	Speed, 80 km/h, tire type 185/65 R15 88H				
Smooth Asphalt	0.0233 (61.322)	0.0025 (41.938)	10.73	0.0133 (56.456)	24.40
Sand	0.0577 (69.207)	0.0025 (41.938)	4.33	0.0404 (66.126)	70.13
Gravel	0.0169 (58.551)	0.0025 (41.938)	14.77	0.0143 (57.101)	84.63

Table 10. The influence of vehicle speeds, on the floor vibration acceleration percentage contribution measured for midsize saloon vehicle and two passengers.

Vehicle speed [km/h]	Floor Vibration Acceleration (FVA), dB ref. 10^{-3}, m/s^2				
	Whole vehicle	Individual sources			
		Engine	Percentage contribution	Tire-road	Percentage contribution
20	0.0106 (20.506)	0.0023 (7.235)	21.70	0.0071 (17.025)	66.98
40	0.0116 (56.258)	0.0024 (41.584)	18.46	0.0076 (51.596)	58.46
60	0.0200 (26.021)	0.002 (6.021)	10.00	0.0090 (19.085)	45.00
80	0.032 (30.103)	0.003 (9.542)	9.38	0.012 (21.584)	37.50
100	0.0332 (30.423)	0.003 (9.542)	9.04	0.006 (15.563)	18.07

Table 11. The influence of vehicle tire type and road surface texture on the floor vibration acceleration percentage contribution measured for midsize saloon vehicle and two passengers.

Road/tire parameters	Floor Vibration Acceleration (FVA), dB ref. 10^{-3}, m/s^2				
	Whole vehicle	Individual sources			
		Engine	Percentage contribution	Tire-road	Percentage contribution
Tire type	Speed, 80 km/h, road surface texture asphalt				
185/65 R15 88H	0.032 (30.103)	0.003 (9.542)	9.38	0.012 (21.584)	37.50
195/60 R15 88H	0.0489 (33.787)	0.003 (9.542)	6.13	0.03890508 (31.800)	18.07
195/65 R15 91H	0.0544 (34.723)	0.003 (9.542)	5.51	0.023669 (31.837)	71.73
Road surface texture	Speed, 80 km/h, tire type 185/65 R15 88H				
Smooth Asphalt	0.032 (30.103)	0.003 (9.542)	9.38	0.012 (21.584)	37.50
Sand	0.0310 (29.827)	0.003 (9.542)	9.68	0.0190393 (25.593)	61.42
Gravel	0.0149 (23.449)	0.003 (9.542)	20.17	0.0090 (19.0931)	60.57

Tables 10 and 11 indicate the broadband averages of floor vibration acceleration (FVA), measured and computed for whole vehicle sources, engine-transmission and tire-road interaction sources for the vehicle speed of 20 km/h to 100 km/h (Table 10), road surface textures and tire types (Table 11) respectively. It is observed that the SPL and FVA originated from the tire-road interaction sources are higher than that originated by engine-transmission sources and both are less than that for complete (whole) vehicle sources in the whole frequency range. Furthermore, from all the SPL frequency domain spectra and in low frequency range below 500 Hz, the interior SPL dominates by the acoustic cavity modes and start to converge roughly above 400 Hz. Therefore, the widely used conventional engine mounts and tires in commercial vehicles cannot fulfill the conflicting requirements for the best isolation concerning both road surface and engine-transmission induced excitations, especially from 31.5 Hz to 80 Hz, where most of these noise and vibration energies are concentrated. Apparently it was not possible to find any tire with equally good noise and vibration performances in this frequency range.

The percentage contribution for both interior noise and vibration originates from tire-road interaction is higher than the one that originates from vehicle engine-transmission system in all the vehicle speed range considered (20 km/h to 100 km/h). On the other hand,

as the vehicle speed is increased from 20 km/h to 100 km/h, the percentage contribution of both engine-transmission and tire-road is decreased with respect to SPL and FVA. This is true because at higher speed the aerodynamic source influence is greater despite some discrepancies in the percentage contribution for SPL only at low vehicle speed (20 km/h). At the vehicle speed of 80 km/h, the percentage contribution from the tire-road and engine-transmission when the vehicle was equipped with a tire type of 195/65 R15 91H and driven on the gravel road surface. These attributed to the level of tire load capacity and index rating, where the gravel road surface texture has the high maximum stone size and overall level.

6. Conclusions

A number of different analysis methods have been discussed, all of which involve capturing the acceleration at the floor and the noise at the driver's head position of the vehicle. Some of the techniques include methods to calculate expected passenger's comfort from the vibration magnitudes measured. Most techniques give results which indicate that the vibration and noise in vehicles are not severe, but could occasionally cause some discomfort.

A basic understanding of the vehicle vibration and noise is necessary to select the reference positions of the sensors and to draw reliable conclusions about the contributions to the response signal. It is also important to perform measurements in all possible operating conditions in order to estimate reliable results.

The values of SPL and FVA broadband averages originate for engine-transmission are lower than that for tire-road interaction. Moreover, the percentage contribution for both interior noise and vibration originates from tire-road interaction is higher than that originate from vehicle engine-transmission system in all the vehicle speed range considered. Furthermore, as the vehicle speed is increased from 20 km/h to 100 km/h, the percentage contribution of both engine-transmission and tire-road is decreased with respect to vehicle interior SPL and FVA.

In this study, a vibration and noise sub-structuring approach of vehicle subsystems of tire-road interaction and engine-transmission were initiated. This sub-structuring approach, once tuned, would allow developing the vehicle vibration and noise properties of the sub-systems separately in parallel, while being able to predict the vehicle vibration and noise properties of the complete vehicle system in the sub-system development phase. Therefore this approach would contribute to reduce the development cycle time of the complete vehicle system

At the vehicle speed of 80 km/h, the percentage contribution from the tire-road and engine-transmission when the vehicle was equipped by a tire type of 195/65 R15 91H and driven on the gravel road surface. These attributed to the level of tire load capacity and index rating, where the gravel road surface texture has high maximum stone size and overall level.

Appendix

$$X = \frac{X_{\text{Ind. Sources}}}{X_{\text{All Sources}}} \cdot 100\%, \tag{4}$$

where X – percent contribution of either Interior SPL or interior FVA, $X_{\text{All Sources}}$ – broadband average of either interior SPL or interior FVA originates from the complete vehicle sources, $X_{\text{Ind. Sources}}$ – broadband average of either interior SPL or interior FVA originates from the individual vehicle sources (i.e. engine or tire-road).

References

1. Abouel-Seoud S.A. (2014), *Assessment of passenger ride comfort during vertical vibration of mid-size saloon and off-road vehicles on asphalt roads*, International Journal of Vehicle Structures and Systems, **6**, 1–2, 39–46.
2. Abouel-Seoud S.A. (2015), *Influence of road roughness parameters on low frequency interior noise in off-road and mid-size passenger vehicles*, International Journal of Vehicle Structures and Systems, **7**, 2, 71–76.
3. Abouel-Seoud S.A. (2016), *Active control analysis of passenger vehicle interior noise produced from tyre/road interaction*, International Journal of Vehicle Noise and Vibration, **12**, 2, 138–161.
4. Abouel-Seoud S.A., Watany M., Elsid M., Abde-Halim N.A., Mohamed E.S., Abdallah A.S. (2018), *Evaluation of vibro-acoustics comfort criterion inside a vehicle manifested from interaction of tire/road*, International Journal of Public Health and Health Systems, **3**, 1, 1–13.
5. Andersen L.G., Larsen J.K. (2015), *Introducing functional data analysis to coast down modeling for rolling resistance estimation*, SAE Journal of Passenger Cars-Mechanical Systems, **8**, 2, 726–732.
6. Gallo M., Komiya Y., Janssens K., Anthonis J., Van der Anweraer H., De Oliveira L.P.R. (2010), *Active sound quality control of vehicle interior sound*, Proceeding of ISMA 2010 including USD2010, pp. 559–570.
7. Junoh A.K., Nopiah Z.M., Abdul A.H., Nor M.J., Ihsan A.K, Fouladi M.H. (2012a), *A study to predict the effects of tires vibration to sound quality in passenger car cabin*, International Journal of Engineering, **6**, 1, 53–69.
8. Junoh A.K, Nopiah Z.M., Muhamad W.Z.W., Nor M.J.M., Fouladi M.H. (2012b), *An optimization model of noise and vibration in passenger car cabin*, Advanced Materials Research, 383–390, 6704–6709.

9. Kim G.-J. (2000), *The identification of tyre induced vehicle interior noise*, Seoul 2000 FISITA World Automotive Congress, June 12–15, Seoul, Korea.

10. Li L., Singh R. (2015), *Start-up transient vibration analysis of a vehicle powertrain system equipped with a nonlinear clutch damper*, SAE International Journal of Passenger Cars Mechanical Systems, **8**, 2, 726–732.

11. Mahajan S.R, Rajopadhye R.D. (2013), *Transportation noise and vibration sources, prediction, and control*, International Journal of Soft Computing and Engineering, **3**, 5, 2231–2307.

12. Mohamed E.S., Abouel-Seoud S.A., Eltantawie M., Mohamud A., Salah M. (2018), *Improved vehicle interior structure-borne noise induced by the powertrain using parallel dry friction damper*, Journal of Low Frequency Noise, Vibration and Active Control, **37**, 2, 295–312.

13. Mohammadi N. (2015), *Analytical and experimental evaluation of cabin noise sources of MB 1924 truck and its acoustic treatment*, International Journal of Engineering and Technology Sciences, **3**, 2, 178–194.

14. Nahvi H., Fouladi M.H., Nor M.J. (2009), *Evaluation of whole-body vibration and ride comfort in a passenger car*, International Journal of Acoustics and Vibration, **14**, 3, 143–149.

15. Nor M.J.M., Fouladi M.H., Nahvi H., Ariffin A.K. (2008), *Index for vehicle acoustical comfort inside a passenger car*, Applied Acoustics, **69**, 4, 343–353.

16. Siano D., Prati M.V., Costagliola M.A., Panza M.A. (2015), *Evaluation of noise level inside cab of a bi-fuel passenger vehicle*, WSEAS Transactions on Applied and Theoretical Mechanics, **10**, 220–226.

17. Sun D., Yan B., Han B., Song Y., Zhang X. (2016), *Vibration characteristic simulation of a pneumatic artificial muscle damping seat*, Journal of Low Frequency Noise, Vibration and Active Control, **35**, 1, 39–51.

18. van der Seijs M., de Klerk D., Rixen D.J. (2016), *General framework for transfer path analysis. History, theory and classification of techniques*, Mechanical Systems and Signal Processing, **68–69**, 217–244.